TRANSNAV the International Journal on Marine Navigation and Safety of Sea Transportation
http://www.transnav.eu
Volume 13
Number 1
March 2019
DOI: 10.12716/1001.13.01.04

Preliminary Inter-comparison of AIS Data and Optimal Ship Tracks

G. Mannarini & L. Carelli
CMCC, Lecce, Italy
D. Zissis, G. Spiliopoulos & K. Chatzikokolakis
Marine Traffic, London, United Kingdom

ABSTRACT: Optimal ship tracks computed via the VISIR model are compared to tracks recorded by the Automatic Identification System (AIS). The evaluation regards 43 tracks in the Southern Atlantic Ocean, sailed during 2016-2017 by different bulk carriers. In this exercise, VISIR is fed by wave analysis fields from the Copernicus Marine Environment Monitoring Service (CMEMS). In order to reproduce vessel speed loss in waves, a new methodology is developed, where kinematic information from AIS is fusioned with wave information from CMEMS. Resulting VISIR tracks are analyzed along with AIS tracks in terms of their topological features and duration. The tracks exhibit quite diverse topological shapes, including orthodromic, loxodromic, and other paths with complex and dynamic diversions. The distribution of AIS to VISIR track durations is analyzed in terms of several parameters, such as the AIS to VISIR track length and their Fréchet distance. Model features of VISIR affecting the results are discussed and future developments suggested by the results are outlined.

1 INTRODUCTION

Global seaborne trade is doing well, but is facing a number of political (inward-looking policies and protectionism), economical (merger and alliances of large shipping lines), and environmental challenges (carbon footprint and sulphur cap) making its long-range outlook quite uncertain[1]. This calls the maritime administrations and industries, among others, for maximizing efficiency of the shipping routes. Shipping routes are specific tracks that vessels follow when traveling between ports and form a global maritime exchange network. Their spatial characteristics are not static though, as over time shipping responds to a number of external parameters. The actual tracks may for instance result from either security reasons (e.g. avoiding risk of exposure to piracy), or economic reasons leading to an optimization process for avoiding rough marine weather (Arguedas et al., 2018). To what extent tracks are already optimized in actual business is not straightforward to assess, but at the same time it would represent an extremely valuable piece of information.

We contribute to this topic via an inter-comparison exercise between reported vessel tracks as collected through the Automatic Identification System (AIS) and tracks planned through the ship route optimization model VISIR. This paper is part of a broader strategy for a comprehensive verification and evaluation of the VISIR ship routing model. The verification (i.e., checking if its equations are solved

[1] https://unctad.org/en/PublicationsLibrary/rmt2018_en.pdf

correctly) included comparison to both static (Mannarini et al., 2016) and time-dependent (Mannarini & Carelli, 2019) analytical solutions as well as comparison to the outcomes of another path planning model (Mannarini et al., 2018). The first step in evaluation (i.e., assessing whether the model fairly represents reality) is presented in this work.

The core of the paper is organized into a description of the evaluation methodology (Section 2) and a presentation of the results (Section 3), which precede conclusive remarks and outline (Section 4).

2 METHODOLOGY

In this Section we describe the methodology employed for this evaluation experiment. The description comprises the extraction of AIS tracks from reported raw data (Section 2.1) and the computation of optimal tracks through VISIR (Section 2.2). The key development enabling the comparison of AIS and VISIR tracks is the computation of the vessel speed loss in waves out of AIS kinematic information, VISIR vessel performance model, and sea state analysis fields (Section 2.3).

Abbreviations and symbols employed throughout this text are defined in Table 1.

Table 1. Some abbreviations and symbols employed in this manuscript.

Symbol	Meaning	Units
SOG	Speed Over Ground	kts
STW	Speed Through Water	kts
COG	Course Over Ground	deg
HDG	Heading	deg
EOT	Engine Order Telegraph	%
UKC	Under Keel Clearance	m
HWHM	Half Width Half Maximum	[-]
L_{wl}	Length at the waterline	m
B_{wl}	Beam at the waterline	m
T_{avg}	Average draught	m
P_{max}	(fitted) maximum engine rating	kW
V_{max}	(fitted) maximum speed in calm water	kts
H_s	Significant wave height	m
α	Wave direction relative to vessel heading	deg

2.1 *AIS tracks*

Nowadays, a multitude of tracking devices and systems produce massive amounts of maritime data on a daily basis. The most commonly used of such tracking systems is the Automatic Identification System (AIS), a collaborative, self-reporting system that allows vessels to broadcast their identification information, characteristics and destination, along with other information originating from on-board devices and sensors, such as location, speed and heading (M.1371, 2014). AIS messages are broadcast periodically and they are received by other vessels equipped with AIS transceivers, as well as by on-ground stations and satellites.

A growing body of literature describes methods of exploiting AIS data for safety and optimisation of seafaring, traffic analysis, anomaly detection, route extraction and prediction, collision detection, path planning, weather routing and many more (Tu et al., 2018). As the amount of available AIS data grows to massive scales though, researchers are realising that computational techniques must contend with difficulties faced when acquiring, storing, and processing the data. Applying traditional techniques to data processing can lead to processing times of several days, if applied to global data sets of considerable size. Additionally, algorithms are challenged by difficulties related to the datasets themselves; including highly skewed, not uniform, and uncertain data. For example, the update interval for AIS is not constant, but dependent on a ship's behaviour; as such it is common for a vessel to broadcast its data every three minutes if moving no faster than 3 knots, while every two seconds if travelling above 14 knots and changing course. In such occasions, the collected positions are spatially and temporally closer. In addition to this, depending on AIS coastal coverage, there are geographical areas where huge amounts of data are collected (e.g. busy ports) while others with much less data. Furthermore, human errors during data entry generate discrepancies for example in naming of ports and areas, generating further uncertainty and ambiguity.

In our previous work (Spiliopoulos et al., 2017), we proposed an efficient big data approach for building a global network of sea routes from AIS data. As a first step of this process we reassign departure and arrival information for each vessel trajectory as although this data is existent in AIS it is error prone and often an issue of confusion. In the present work we consider vessel trajectories travelling between the ports of Buenos Aires (Argentina) and Port Elizabeth (South Africa) from July 2016 until the end of December 2017. These trajectories amounted to more than 160,000 AIS messages in total. Each of these messages consists of the coordinates of the vessel transmitting the message, the corresponding kinematic characteristics of the vessel (such as SOG, COG, and HDG), and a timestamp. For identification purposes an anonymised vessel's identifier and voyage data are bound to each message.

Within this dataset, we identified 61 different trajectories in total, each of them being performed by a different vessel. Moreover 51 of these trajectories correspond to dry bulk carriers and the remaining 10 trajectories to wet bulk carriers. For each voyage, the vessel's dimensions, engine power and maximum historical speed information were included in our analysis. The summarised characteristics of the anonymised vessels in this dataset are shown in Table 2.

Table 2. Vessel characteristics. μ and σ stand for average and standard deviation of the vessel sample.

		Dry bulk	Wet bulk
Number of vessels		51	10
Length [m]	μ	201	182
	σ	19	2
Width [m]	μ	32	31
	σ	2	2
Engine Power [kW]	μ	8600	9000
	σ	1500	2200
Max Speed [knots]	μ	12	12
	σ	2	3

2.2 *VISIR tracks*

VISIR (an acronym for "discoVerIng Safe and effIcient Routes") is the ship routing model resulting from the prototype first published in Mannarini et al. (2013). The model eventually evolved to compute least-time tracks in presence of time-dependent fields from wave models (Mannarini et al., 2016), and has been recently extended to deal also with ocean currents in Mannarini et al. (2019).

VISIR is based on a graph-search algorithm, with graph edges accounting for vessel COG, and edge weights depending on the sailing time between graph nodes. Graph edges crossing the landmass are pruned, enabling computation of tracks even in coastal waters or in vicinity of islands. Furthermore, vessel intact stability can be accounted for through checks on parametric roll, pure loss of stability, or surfriding/broaching-to (IMO, 2007). Either intentional speed reduction (EOT<1) or course change can be exploited by VISIR for fulfilling the stability constraints.

2.2.1 *Path planner setup*

For this actual evaluation experiment, the VISIR model configuration is described through the parameters provided in Table 3. The graph resolution parameters are chosen to compromise between spatial and angular accuracy on the one hand and computational effort on the other one. UKC is not checked in this exercise, as the employed GEBCO bathymetry[2] would not allow, for the actual vessel draught, a UKC>0 at the Western end of the AIS tracks (located at the estuary of Rio de la Plata, in South America).

Safety constraints and intentional speed reduction are also disabled as, according to Mannarini et al. (2019), for this actual route, they do not to significantly impact the results. Conversely, disabling them allows reducing the computer RAM allocation of the computations and, thus, increasing the maximum number of time steps considered for VISIR paths. In fact, the vessel type considered in this experiment is (both dry and wet) bulk carrier, which top speeds (Table 2) are generally lower than container ships considered instead in Mannarini et al. (2019). A lower speed implies a longer sailing time, which is represented in VISIR through a larger number of time steps and, thus, requires higher RAM allocation.

Table 3. VISIR configuration for the computations of this experiment.

Feature	Value
Grid resolution	1/7 deg (= 8.6 nmi in meridional direction)
Angular resolution	8.1 deg
Ocean currents	neglected
Safety constraints	shoreline only, UKC>0 and intact stability checks disabled
Intentional speed reduction	disabled

[2] https://www.gebco.net/data_and_products/gridded_bathymetry_data/)

For the same reason, ocean currents are neglected in this first version of the evaluation experiment. The role of this approximation with respect to the self-consistency of the whole methodology is discussed in Section 2.3.1.

Finally, CMEMS[3] three-hourly wave fields are averaged into daily fields before being employed by VISIR. Again, as discussed in (Mannarini et al., 2019), the reason for this approximation is the reduction of RAM allocation.

2.3 *Vessel response function*

As mentioned above, the critical modeling piece for the evaluation of VISIR vs. AIS tracks is the vessel response function. It defines the involuntary speed loss in waves due to the added resistance R_{aw} (Bertram and Couser, 2014). Because of speed loss, path diversions may allow sailing at an higher speed than along the least-distance track. Thus, by taking a diversion, destination may be reached earlier. Since the objective of the track optimization is to minimize such a sailing time, diversions that optimally compromise between reduced speed loss and increased track length are chosen by the algorithm.

The vessel response function is defined within VISIR as the STW sustained at specific values of significant wave height H_s (Mannarini et al., 2016). Its functional form is obtained from a power balance at the ship propeller and makes use of a parametrization of R_{aw} based on a statistical reanalysis of numerical simulations via the Gerritsma and Beukelman's method (Alexandersson, 2009). The parametrization depends on just three main geometrical parameters: vessel length L_{wl}, beam B_{wl}, and draught T_{avg}. When applied to the VISIR power balance, it results into a Gaussian-shaped vessel response function, with a peak value given by vessel top speed in calm water V_{max} and a HWHM proportional to maximum engine break power P_{max}.

The dependence on wave direction (relative to vessel heading) is presently neglected within the VISIR vessel model. The impact of this approximation is discussed in the subsection below.

2.3.1 *Developments for the current experiment*

For the current evaluation experiment, the five parameters (L_{wl}, B_{wl}, T_{avg}, P_{max}, V_{max}) needed for computing the vessel response function are identified in the following way:

1 Hull geometry parameters (L_{wl}, B_{wl}, T_{avg}) correspond to the vessel details identified through the IMO-number provided along with the AIS record;
2 Propulsion and performance parameters (P_{max}, V_{max}) are fitted to the data of speed loss in waves, generated as in the following.

A speed loss diagram (scatter plots of SOG vs. corresponding H_s experienced by the vessel) is first produced.

[3] http://marine.copernicus.eu/

H_s is not part of the AIS record. However, it can be estimated from sea state model analysis. Analyses are the best available reconstructions of an environmental state, making use of both observations and geophysical model outputs. We employ CMEMS analysis fields which assimilate observations of significant wave height from Jason 2 & 3, Saral and Cryosat-2 altimeters into the MFWAM sea state model[4]. For each AIS track leg, we extract the spatially and temporally nearest CMEMS gridpoint value. This value represents our best estimation of H_s encountered by the vessel at that specific AIS spatial location and time.

Resulting data of speed loss in waves are displayed in Figure 1, where they are plotted vs. either H_s or relative wave direction α. Despite the fact that, even for a specific vessel, data are strongly scattered, a general trend for speed loss with increasing H_s is recognized. Also, maximum loss is achieved for head waves. This is consistent with calculations and towing tank data of wave added resistance provided by Tsujimoto et al. (2013).

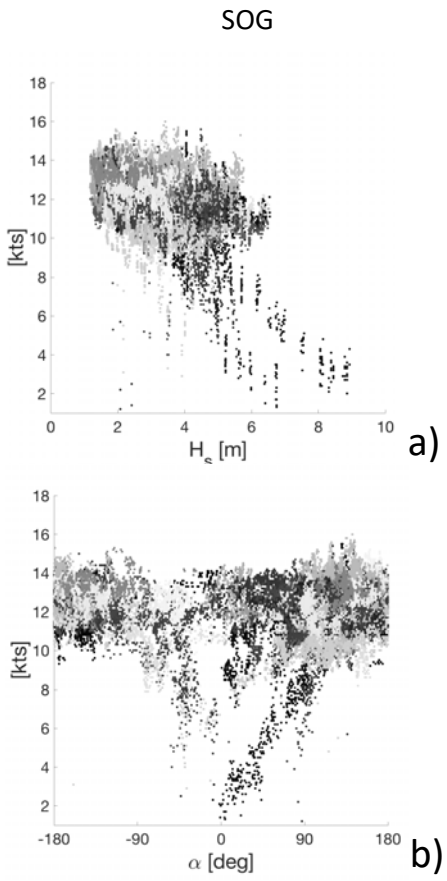

Figure 1. Speed loss in waves out of AIS kinematic data and CMEMS sea state fields. Panel a) displays the dependence on significant wave height, while b) the dependence on wave-vessel relative direction (α = 0 deg means head seas, α > 0 refer to waves from the starboard). Marker grey tones refer to individual voyages/vessels.

Datapoint scattering in Figure 1 can be attributed to:

1 neglect of ocean currents, which combines with STW for producing SOG;
2 limited skill of the CMEMS analysis fields in the reconstructing the sea state.

The difference between SOG and STW, being related to ocean current magnitude and direction (Mannarini & Carelli, 2019), can be as high as several knots. However, identifying STW with SOG is consistent with the fact that, for this experiment, we are neglecting ocean currents also for the computation of VISIR optimal tracks. A more accurate treatment is planned for future developments of this evaluation methodology.

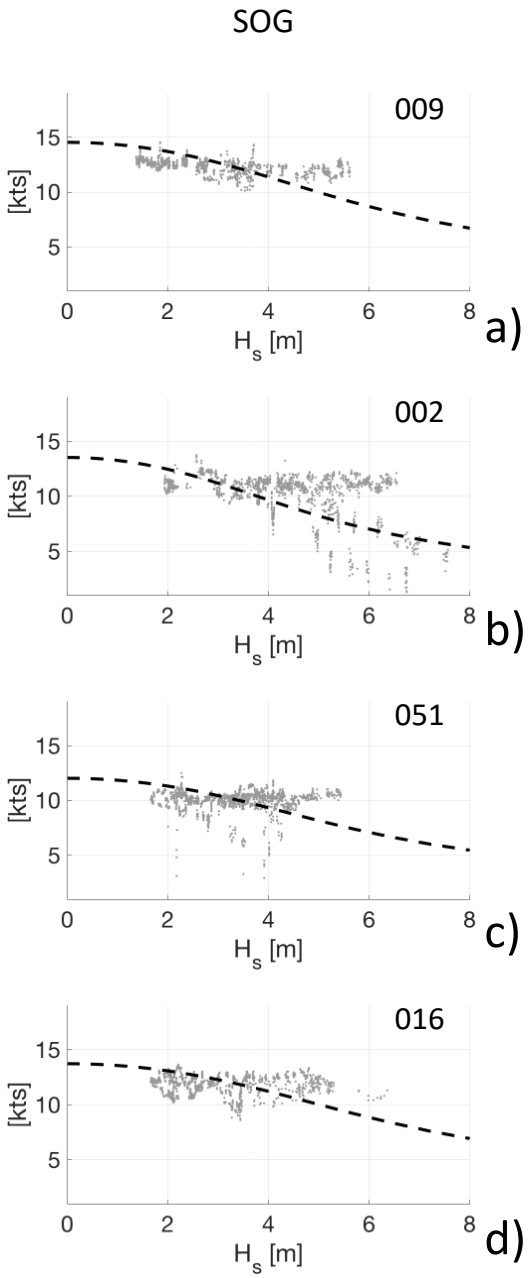

Figure 2. SOG dependence on significant wave height. AIS data are represented as gray dots, while the VISIR response function for fitted P_{max} and V_{max} parameters is shown as a dashed line. Each panel refers to a different voyage/vessel, identified by the 3-digit code in the top-right.

Both the response function resulting from AIS kinematical data and CMEMS wave fields and the fitted VISIR speed loss curves are displayed in Figure 2 for selected vessels. The data have been previously

[4] http://cmems-resources.cls.fr/documents/PUM/CMEMS-GLO-PUM-001-027.pdf

filtered by pruning data in the vicinity of the track endpoints (harbours). There, due to vessel acceleration, SOG can strongly vary even in correspondence of a constant H_s value.

VISIR speed loss curve generally fits well to the data, but in the case when they include more than a branch at larger H_s. If this is the case, the VISIR curve is fitted in between the branches (Figure 2b).

The presence of multiple speed loss branches may be due to vessel performance in head waves, which are not accounted by the present ship model. In some cases, even a speed increases with H_s is observed (Figure 2d), which may be due either to EOT changes or to ocean currents.

In Fujii et al. (2017) too, a speed loss curve out of AIS and model wave data is displayed. The authors considered tracks of container ships and pure car carriers in the North Pacific. However, their data do not support a clear relation between SOG and H_s.

Finally, we note that the information in step b) of the present procedure just represents the P_{max} and V_{max} fit parameters and does not necessarily agree with the actual vessel parameters for maximum engine brake power and speed.

3 RESULTS

In this Section, results relative to systematic application of the methodology of Section 2 to transatlantic passages between Buenos Aires (Argentina) and Port Elizabeth (South Africa) and vice-versa during the years 2016 and 2017 are presented and discussed. The results for a few individual tracks (Section 3.1) precede the analysis of the ensemble of the tracks from the topological viewpoint (Section 3.2) and by investigation of the dependence of track duration on several variables (Section 3.3).

3.1 *Individual tracks*

A one-to-one comparison of VISIR to AIS track topology is displayed for a selection of all the voyages in Figure 3.

The tracks are portrayed on top of the CMEMS wave fields. The latter are generally taken at the timestamps of the AIS waypoints and displayed as adjacent vertical stripes. VISIR instead employs daily averages of the CMEMS waves. These are shown in Figure 3.b-c in the portion of the map containing the VISIR trajectory.

Finally, each panel displays also the geodetic track computed by VISIR. This track is, in the open ocean, an arc of great circle joining the track endpoints. In that case, it is identical to the orthodromic path. The main features of the various panels of Figure 3 are described in the following:

1 For this ship voyage, both VISIR and AIS tracks take an initial Northbound diversion and then sail to destination along a trajectory close to the loxodromic (i.e., constant bearing) path. The diversion is slightly anticipated by VISIR, which in the second part of the voyage computes a diversion approaching the geodetic track.
2 A significant track disagreement is noticed, with AIS close to orthodromic navigation and VISIR taking a wide Northbound diversion. VISIR diversion is instrumental in avoiding the rough seas between 25-10°W and 5-15°E. This corresponds to the second part of the voyage, at 6 and 12 days since departure respectively. AIS track may result from the fact that the rough sea in the second part of the voyage could not be exactly forecast at the time of departure.
3 AIS track diverts North while VISIR track diverts even South of the geodetic. The different wave field stripes in the upper and lower part of the map make clear that the diversion computed by VISIR is instrumental in avoiding rough seas at the latitude of the geodetic and above.
4 Both AIS and VISIR tracks sail a path between the rhumb-line and the least-distance track. VISIR track is closer to the latter in vicinity of both departure and arrival locations, resulting in a shorter track length than AIS data.

In both Figure 3.b-c an appreciable difference between three-hourly and daily-averaged wave fields can be noticed. The observed divergent AIS and VISIR trajectories might be ascribed to this fact.

3.2 *Tracks ensemble topology*

The original 61 AIS tracks were reduced to 43 due to the fact that some tracks presented an anomalous length or that the response function, upon spatial pruning, contained too few datapoints. Each of the 43 voyages in the AIS record is sailed by a different vessel, for which a speed loss curve was computed as described in Section 2.3.1.

It is employed for computing an optimal track via VISIR between the actual AIS endpoints, for their specific departure date and time.

In Figure 4 all Eastbound tracks from both AIS and VISIR between July 31 2016 and December 13, 2017 are displayed. The tracks form a bundle with an appreciable meridional extent. In the middle of the passage, the bundle extent is about 12° for AIS and about 20° for VISIR, which bundle extends even South of the geodetic track. For both AIS and VISIR, there is a general trend to larger diversions for tracks sailed during (Southern hemisphere) winter months. A significant meridional dispersion of the AIS tracks is also noticed in the data published by Fujii et al. (2017).

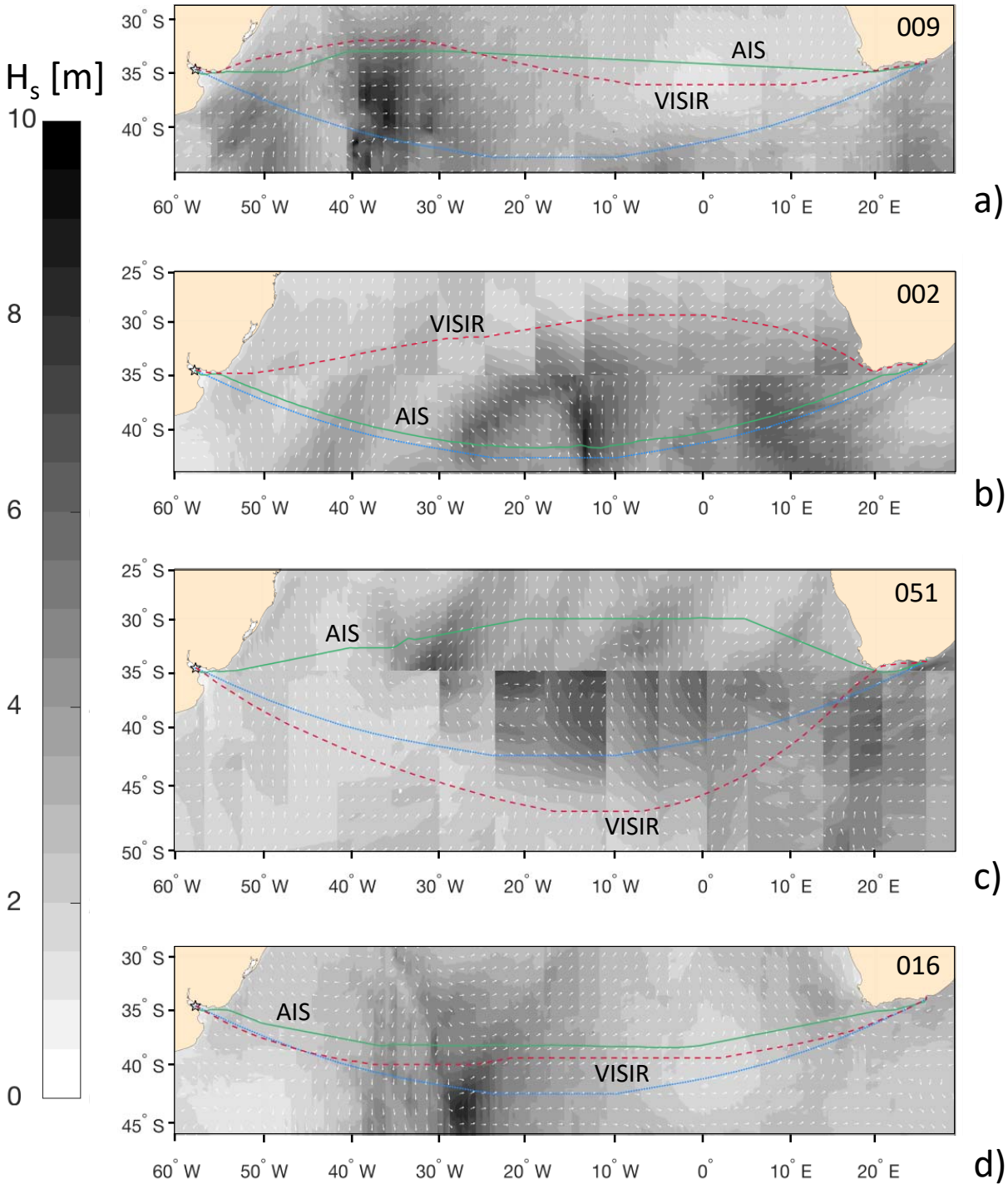

Figure 3. Tracks of voyages referenced also in Figure 2 displayed on top of CMEMS three-hourly wave fields. The white arrows denote wave direction. In each panel, AIS, VISIR, and geodetic tracks are displayed as a green solid line, a red dashed line, and a blue dotted line respectively. Panels b) and c) are split vertically, with the daily-averaged wave fields displayed in correspondence of the VISIR tracks and the three-hourly fields in correspondence of the AIS tracks.

3.3 *Tracks ensemble – key metrics*

The track ensemble is also analyzed in terms of track duration (sailing time), which is the optimization objective for VISIR. Track duration could be the guiding principle for shipmaster decisions as well, since costs relative to bunker and onboard personnel are proportional to duration.

First of all, durations of VISIR optimal tracks (T_V) are compared to durations on the geodetic track (T_G). They are computed by VISIR accounting for speed loss in waves. Figure 5a confirms that VISIR's optimization works as expected, saving up to about two days with respect to orthodromic navigation.

T_V are also compared to AIS durations (T_A) in Figure 5b, finding $T_V < T_A$ always. Again, VISIR savings exceed two days in some cases.

In order to get a deeper insight on the reasons for the better performance of VISIR, the relative duration saving - Δ_{va} of VISIR to AIS trajectory ($\Delta_{va} = T_V/T_A - 1$) is displayed in Figure 6. in dependence of four different variables:

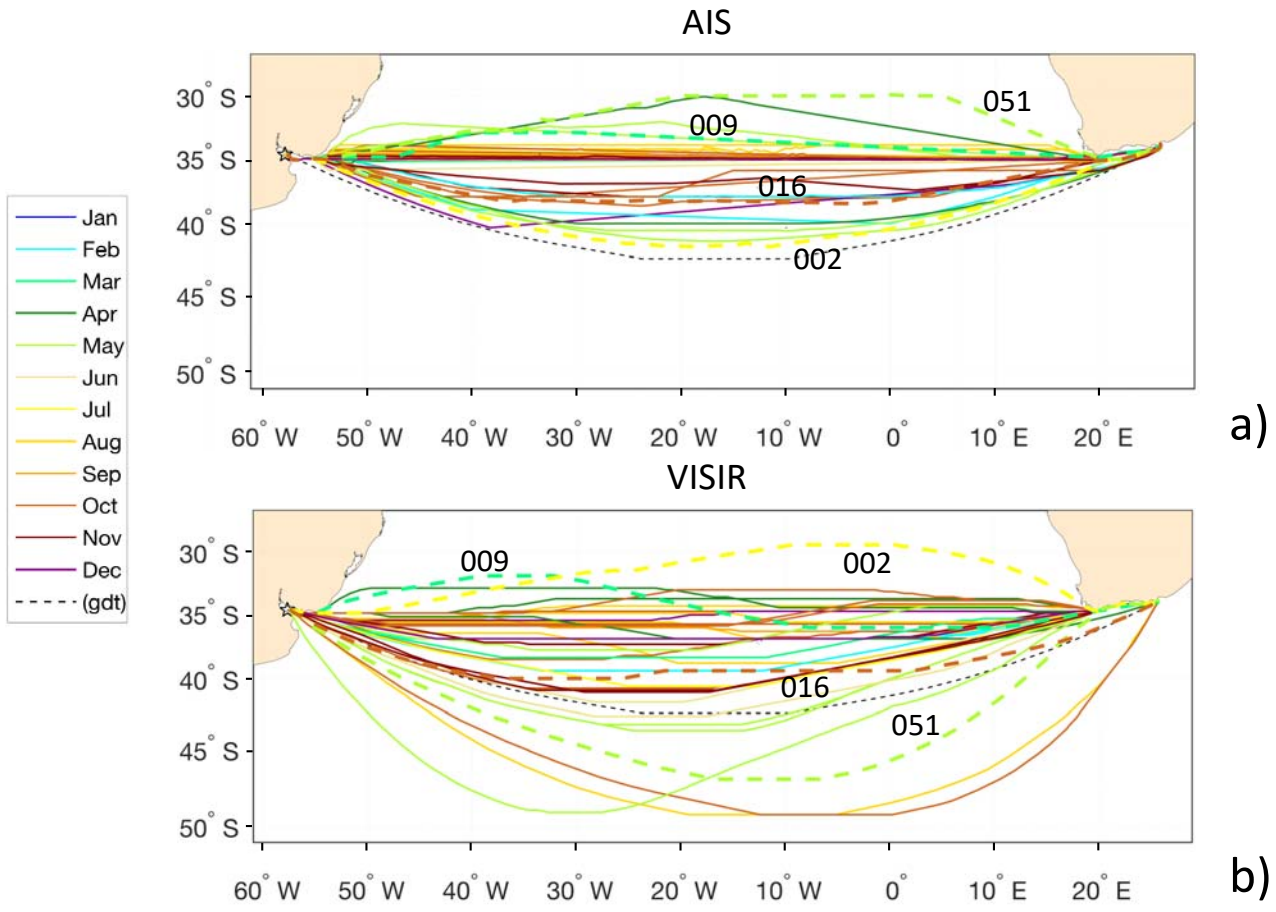

Figure 4. Route departing from Buenos Aires (Argentina) arriving in Port Elizabeth (South Africa). a) displays AIS tracks, while b) shows VISIR simulations departing on the same dates. Dashed bold tracks with numeric labels refer to the selected voyages referenced also in Figure 2.

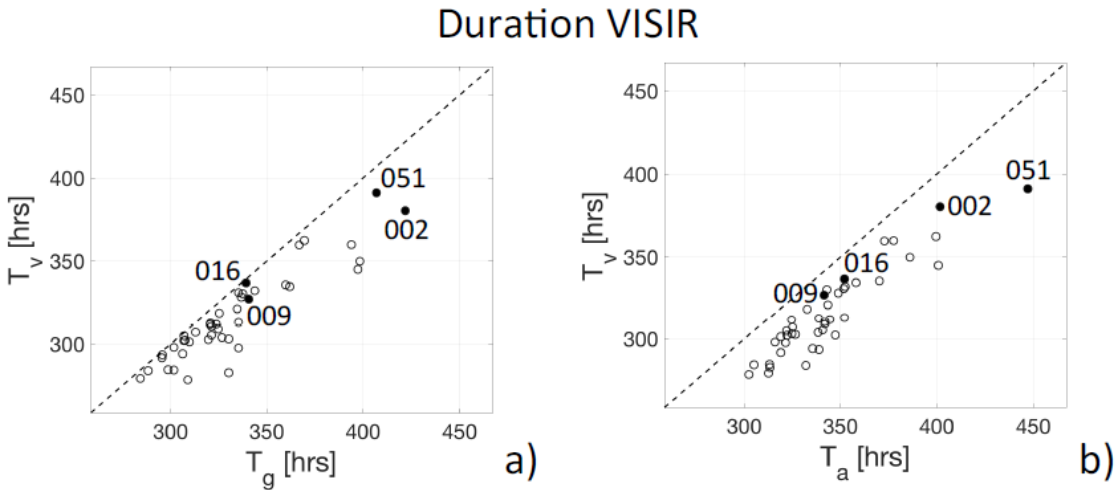

Figure 5. Analysis of VISIR optimal track durations T_V. Panels a) and b) compare to the duration of VISIR geodetic T_G and AIS tracks T_A respectively. In every panel, the codes of the voyages are put in evidence, which speed losses in waves are displayed in Figure 2.

Vessel maximum speed (fit parameter V_{max}). There possibly is some correlation between Δ_{va} and V_{max}. This is one of the fit parameters in Figure 2 and is related but not identical to the actual vessel top speed. This trend should be confirmed by a larger track statistics;

The length ratio of AIS to VISIR tracks (L_A/L_V). It is close to unity with a high precision (within 5%) in most cases. When departing from unity, a trend of -Δ_{va} increasing with L_A/L_V seems to be supported by the data;

1 The month of departure of the track. No clear seasonal trend is recognized, but a larger -Δ_{va} variability in (Southern Hemisphere) summer months. Before making hypothesis on its origin, the statistics should be enlarged;

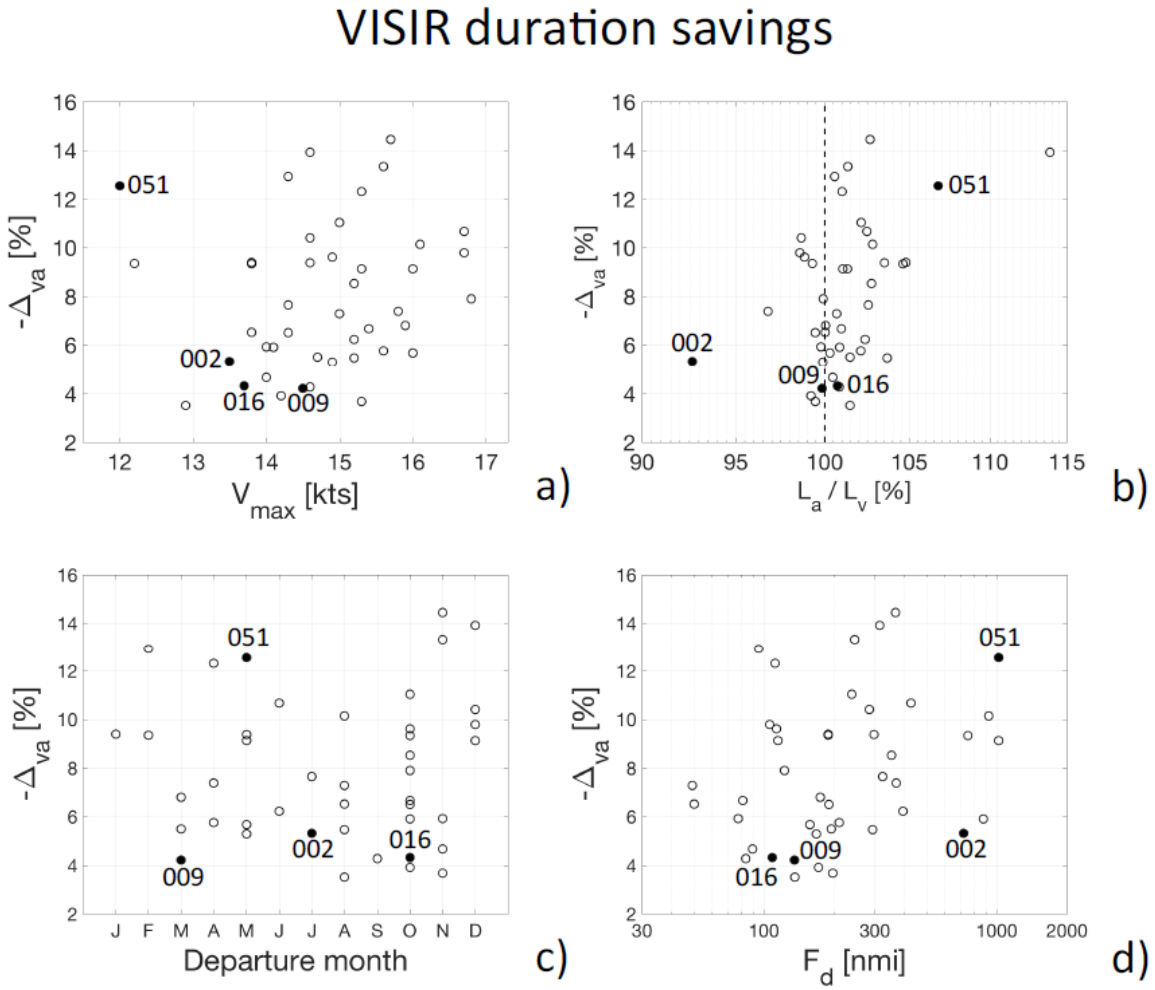

Figure 6. Analysis of relative VISIR to AIS track duration savings $-\Delta_{va} = 1 - T_V/T_A$ with respect to several parameters. Panel a) displays the dependence on the V_{max} fit parameter; b) dependence on the AIS to VISIR track length ratio L_A/L_V; c) dependence on month of departure; d) dependence on Fréchet distance F_d between VISIR and AIS tracks. In every panel, the codes of the voyages are put in evidence, which speed losses in waves are displayed Figure 2.

2 The Fréchet distance[5] F_d, representing VISIR and AIS track similarity. It seems that the maximum $-\Delta_{va}$ increases with F_d, but the data are quite scattered.

4 CONCLUSIONS

We have completed a preliminary evaluation of VISIR ship routing model with respect to vessel tracks reported through AIS data. The evaluation has included the development of a new methodology for determining speed loss in waves from fusion of empirical data (AIS) and meteo-oceanographic model output (wave analysis fields). A case study of 43 voyages in the Southern Atlantic Ocean has been considered. The results indicate that:

1 VISIR track topology generally agree well with AIS one, though in some cases completely different tracks, with a large Fréchet distance from AIS, are computed;
2 There is a significant annual variability of the spatial structure of the tracks, both in the AIS records and in the VISIR simulations. A number of AIS tracks are close to the loxodromic track and the VISIR tracks at times extend even South of the orthodromic track;
3 VISIR sailing times are always shorter (4-14%) than AIS ones, while their total length remains quite close to the AIS one in most cases;
4 VISIR time savings are larger for AIS tracks longer than VISIR ones. Furthermore, the duration savings could also be related to top vessel speed and seems to vary most during (Southern Hemisphere) summer months.

These conclusions are supportive of the fact that some kind of optimization (either automated or manual) took place in most of the actually sailed tracks.

Discrepancies between VISIR and AIS both in terms of duration and spatial structure can be ascribed to at least two factors:

1 VISIR model features and approximations. For this first exercise:
  – three-hourly wave fields have been averaged into daily fields, for the sake of reducing the computer RAM allocation, cf. Mannarini & Carelli (2019). As noted in Section 3.1, this may be one of the reasons for the larger discrepancies between AIS and VISIR tracks;

[5] http://www.kr.tuwien.ac.at/staff/eiter/et-archive/cdtr9464.pdf

- ocean currents have not been considered, neither for the optimal track computation, nor for reconstructing STW out of SOG;
- a directional wave response is not yet modeled. Its impact depends on how the a-directional VISIR response function was fitted to the AIS-CMEMS data in Figure 2. Whenever VISIR curve is adjusted to the steepest branch of the data, its speed loss is overestimated to always be the one relative to head waves. On the other hand, adjusting to the most constant branch would underestimate the speed loss in head wave. Overestimation of speed loss would induce an overestimation of the spatial diversion along the optimal tracks;

2 Unavailability, for the ship officer in charge of track planning, of long enough wave forecasts. Since forecasts are usually limited to a few days lead time (e.g. 5 days for CMEMS[6], 7.5 days for NCEP[7]), a sub-optimal track may result from this fundamental knowledge gap at the time of vessel departure. This is especially relevant when rough seas are encountered several days after departure (cf Figure 3.b,c). This may induce a conservative approach by the shipmaster, for instance avoiding diversions towards circumpolar latitudes (cf Figure 4). VISIR tracks instead, employing reconstructions of the sea-state (analysis fields), are not affected by this fundamental limitation.

We consider these preliminary results quite encouraging. A larger track statistics and consideration of routes in other parts of the global ocean should enable an even deeper insight into optimization choices by actual vessels. Also, this approach provides further indication of what VISIR model features need to be developed more urgently.

ACKNOWLEDGEMENTS

This work has received funding from the European Union Horizon 2020 research and innovation programme under grant agreements No. 633211 (AtlantOS) and No. 732310 (BigDataOcean) and the Italy-Croatia Interreg V-A programme under project ID 10043587 (GUTTA).

REFERENCES

Alexandersson, M. *A study of methods to predict added resistance in waves*. Master's thesis, KTH Centre for Naval Architecture, 2009.

Arguedas et al. 2018. Maritime Traffic Networks: From historical positioning data to unsupervised maritime traffic monitoring. IEEE-ITS, 19(3): pp.722732.

Bertram V. and Couser. P. 2017. Computational methods for seakeeping and added resistance in waves. In B. Volker (ed.), *13th International Conference on Computer and IT Applications in the Maritime Industries, Redworth, 12-14 May 2014, pages 8–16*. Harburg: Technische Universität Hamburg.

Fujii M., Hashimoto H., Taniguchi Y. 2017: Analysis of Satellite AIS Data to Derive Weather Judging Criteria for Voyage Route Selection. *TransNav, the International Journal on Marine Navigation and Safety of Sea Transportation*, Vol. 11, No. 2, doi:10.12716/1001.11.02.09, pp. 271-277

IMO. MSC.1/Circ.1228 Revised guidance to the Master for avoiding dangerous situations in adverse weather and sea conditions. Technical report, International Maritime Organization, London, UK, 2007.

M.1371: Technical characteristics for an automatic identification system using time-division multiple access in the VHF maritime mobile band." [Online]. Available: https://www.itu.int/rec/R-REC- M.1371/en

Mannarini G., Coppini G., Oddo P. and Pinardi N. 2013. A prototype of ship routing decision support system for an operational oceanographic service. *TransNav, the International Journal on Marine Navigation and Safety of Sea Transportation*, 7(1): 53–59.

Mannarini G., Pinardi N., Coppini G., Oddo P. and Iafrati A. 2016. VISIR-I: small vessels – least-time nautical routes using wave forecasts. *Geoscientific Model Development*, 9(4): 1597–1625. https://www.geosci-model dev.net/9/1597/2016/gmd-9-1597-2016.pdf

Mannarini G. & Carelli L. 2019. VISIR-I.b: waves and ocean currents for energy efficient navigation. *Geoscientific Model Development Discussions*, (under review)

Spiliopoulos, G., Chatzikokolakis, K., Zissis, D., Biliri, E., Papaspyros, D., Tsapelas, G. and Mouzakitis, S. 2017. Knowledge extraction from maritime spatiotemporal data: An evaluation of clustering algorithms on Big Data. In Big Data (*Big Data*), *2017 IEEE International Conference on* (pp. 1682-1687). IEEE.

Tu E., Zhang G., Rachmawati L., Rajabally E., and Huang G. B. 2018, Exploiting AIS Data for Intelligent Maritime Navigation: A Comprehensive Survey From Data to Methodology. *IEEE Trans. Intell. Transp. Syst.*, vol. 19, no. 5, pp. 1559–1582.

Tsujimoto, M., Kuroda, M. and Sogihara, N. 2013. Development of a calculation method for fuel consumption of ships in actual seas with performance evaluation. In ASME 2013 32nd International Conference on Ocean, Offshore and Arctic Engineering (pp. V009T12A047-V009T12A047). American Society of Mechanical Engineers

[6] GLOBAL_ANALYSIS_FORECAST_WAV_001_027

[7] https://polar.ncep.noaa.gov/waves/product_table.shtml?-hs-multi_1-atlantic-latest-